The effect of wakes on the fatigue damage of wind turbine components over their entire lifetime using short-term load measurements

Sarah Karlina-Barber, Sebastian Mechler and Mario Nitschke

Fraunhofer IWES, Am Seedeich 45, 27572 Bremerhaven, Germany

sarah.karlina-barber@iwes.fraunhofer.de

Abstract. A method is developed for quantifying the effect of neighboring wind turbines on the fatigue damage of the main components of a wind turbine over its entire operating time using short-term load measurements. This method could be used in the future for improving wind farm planning software that takes into account fatigue damage as well as energy yield or for improving lifetime extension calculations of wind turbines. The method is applied here to a measurement campaign on a Vestas V66 wind turbine located in northern Germany and the results are found to be plausible. Furthermore, the results show that the increase in total lifetime fatigue damage due to neighboring wind turbines for wind turbine separations of the order of 5D is significant and needs to be taken account of in wind farm planning software. The accuracy of the method is examined by investigating the sensitivity of the main assumptions on the results. It is found to be strongly dependent on the number of measured time-series in a wind speed bin as well as on the choice of wind speed frequency distribution. The method therefore needs to be standardized before it is applied to improving wind farm planning software or lifetime extension calculations of wind turbines.

1. Introduction and objectives

Measuring the mechanical loads acting on the key components of wind turbines together with the wind conditions and the operating parameters is a well-established method for assessing performance. For the type certification of a new wind turbine model, the mechanical loads must be measured based on the international standard IEC 61400-13 [1]. These measured loads are then compared to the design calculations. They have the potential to reveal a large amount of highly detailed, quantitative information about the performance of a wind turbine; however, the analysis demanded in the standard is fairly limited. The captured data could be exploited for many other applications, such as to improve the understanding of the effects of neighboring wind turbines on the damage of the components and for establishing the potential lifetime extension of wind turbines.

Improving the understanding of the effects of neighboring wind turbines on the damage of the components is important especially due to the recent pressure on wind farm operating costs [2] and reduced space [3] as well as due to the fact that installed wind turbines are getting older. Wind farm planning software such as WindPRO [4] and WindFarmer [5] currently use wake models that only account for wind speed reductions and not for increased fatigue damage. The general rule-of-thumb for allowable wind turbine separation is five to seven rotor diameters (5-*8D*) in the main wind direction and 2-5*D* in crossflow, for which the resulting fatigue damage over the lifetime of the wind

turbines is assumed not to be affected (depending on the source, e.g. [6], [7], [8], [9]). The need for replacing this rule-of-thumb assumption with a fatigue damage model has been discussed since 1999 [10] and has been studied in various field measurement campaigns [11]. Recently, load measurements have been applied for investigating the effects of neighboring wind turbines on the damage of the components [3], [12]; however, only in terms of the increased damage equivalent loads and not in terms of the increased lifetime fatigue damage.

Establishing the potential lifetime extension of wind turbines is becoming increasingly important as installed wind turbines get older. Currently, approximately 28% of the 16,000 installed wind turbines in Germany are over 15 years old [13]. For establishing the potential lifetime extension of wind turbines, a visual inspection and an analytical part is currently required [14]; however, no measurements at the site are used, mainly due to the high costs of such measurement campaigns. In order to establish the potential lifetime extension of a wind turbine correctly, however, the actual loads on the components have to be measured. Methods involving shorter-term measurements and examination of the resulting load spectra have been investigated recently [15], showing that the potential error in calculating the lifetime extension of wind turbines without measuring the loads is significant, especially when the wind turbine is located within a wind farm.

In this work, a complete set of mechanical load measurements based on IEC 61400-13 [1] is carried out over a period of eight months on a Vestas V66 1.65 MW wind turbine located in north-western Germany. The wind turbine was installed in December 2001 and is affected by two neighboring Enercon E-70 wind turbines, which were installed upstream of the measured wind turbine in the main wind direction in January 2006. The goal of this work is to develop a method to quantify the effect of the neighboring wind turbines on the fatigue damage of the main components of the measured wind turbine over its entire operating time using short-term load measurements. This method could be used in the future for improving wind farm planning software that takes into account fatigue damage as well as energy yield or for improving lifetime extension calculations of wind turbines.

2. Mechanical load measurements

2.1. Measurement system

The mechanical load measurements were carried out according to IEC 61400-13 [1] between November 2014 and June 2015 on a Vestas V66 1.65-MW wind turbine belonging to the wind farm operator *Projektierungsgesellschaft für regenerative Energiesysteme mbH*, Oldenburg, Germany. The wind turbine has a hub height of 67 m and a rotor diameter of 66 m. The main wind direction is approximately south-west.

Full-bridge strain gauges were installed on the blade root, the main shaft, at the tower top and at the tower bottom of the V66 in order to measure the bending moments in two perpendicular directions. V-shaped strain gauges were additionally installed on the main shaft and tower top in order to measure the torsion. The strain was measured at a frequency of 100 Hz using calibrated amplifiers installed in cabinets at the tower top and tower bottom. A telemetry system was used in order to transfer data from the rotating systems in the hub and on the main shaft to the nacelle. Additionally, the blade pitch, rotor position, rotor speed, yaw position and power were measured using sensors connected to the same measurement system. The entire system was connected to a data logger in the tower bottom via fiber-optic cables. The measurements were synchronized using a GPS time server. The system was calibrated once installed on the wind turbine using a combination of measurements in low wind conditions and an analytical method according to IEC 61400-13 [1]. The measurements were corrected for drift and the total measurement uncertainties ranged from 3%-7%, dependent on load quantity.

Wind measurements were undertaken using a 30 m met mast, a Leosphere WINDCUBE v2 LiDAR and the wind turbine SCADA data. The sensors on the met mast were all installed according to 61400-12-1 [16], with the exception that the mast was too short (for comparisons with LiDAR measurements it should be either at least 40 m high or at least as high as the bottom of the rotor, in this

case 34 m). In previous work, the reliability and validity of this set-up was investigated thoroughly [17]. This included the development of a transfer function between the ten-minute averaged SCADA wind speed data and the LiDAR hub-height data according to IEC 61400-12-2 as well as a correction of the measured yaw angle using a comparison with the measured LiDAR wind direction [18]. This wind speed transfer function and yaw angle correction are applied in the present work because the met mast data does not cover the entire measurement period.

The positions of the measured and neighboring wind turbines as well as the met mast and the LiDAR are shown in Figure 1 (view from above). The relevant wind direction sectors, calculated according to the obstacle analysis method in IEC 61400-12-1 [16] are shown in Figure 2. The wind rose also shown in Figure 2 was provided by the operator. The neighboring wind turbines are located at a distance of 3.6*D* and 6.2*D* from the V66.

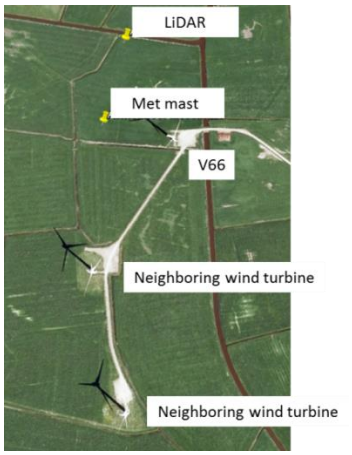

Figure 1. Layout view of the wind park situation from Google Maps.

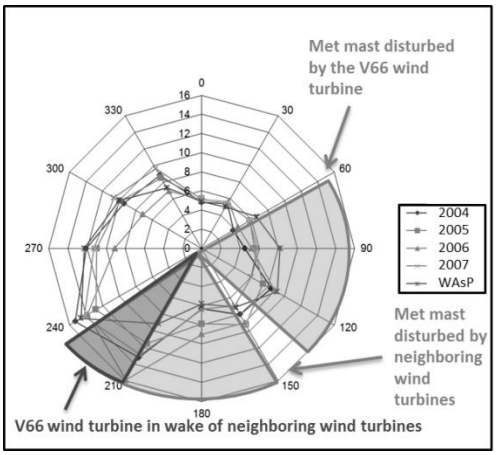

Figure 2. Sector analysis for the V66.

2.2. Measurement results

The main outputs of the mechanical load measurements are the distributions of ten-minute averaged loads and 1 Hz damage equivalent loads with wind speed during normal operation as well as their bin-averages for wind speed bins. The 1 Hz damage equivalent load (DEL) is defined as the amplitude of the load that would have had to act on the component with a frequency of 1 Hz in order to cause the same damage as the acting load.

The DELs for each ten-minute time series are calculated for each load quantity by firstly rainflow-counting the load quantity time series into range bins. Then the rainflow-cycle counts of individual ten-minute records are assembled to form a single cumulative rainflow-spectrum for power production. This is done by summing all the individual rainflow-cycle counts of each file in the power production capture matrix. The DEL for a single ten-minute time series, *j*, is then calculated as follows [1]:

$$DEL_j = \left(\frac{\sum R_i^m n_i}{600}\right)^{1/m} \quad (1)$$

where R_i = load of the *i*-th range bin of the fatigue load spectrum, n_i = number of cycles in the *i*-th range bin of the fatigue load spectrum, *600* = 60 seconds × 10 minutes cycles and *m* = S-N-curve slope for the relevant material (4 for welded steel and 10 for glass-fiber-reinforced plastic). The S-N curve is a standard approximation for fatigue and is given in general by [19]:

$$N = CS^{-m} \tag{2}$$

where N = number of cycles to failure, S = load range level and C and m are material properties.

The ten-minute averaged DELs and the corresponding standard deviations calculated from the measured loads in this project are shown for the tower bottom lateral bending moment as a function of hub-height wind speed in Figure 3. An example of the bin-averaged DELs for the tower bottom lateral (*M_tbl*) and normal (*M_tbn*) bending moments is shown in Figure 4 (where normal refers to the direction perpendicular to the wind direction). This behavior is as expected due to the increasing amplitude of load cycles above rated wind speed.

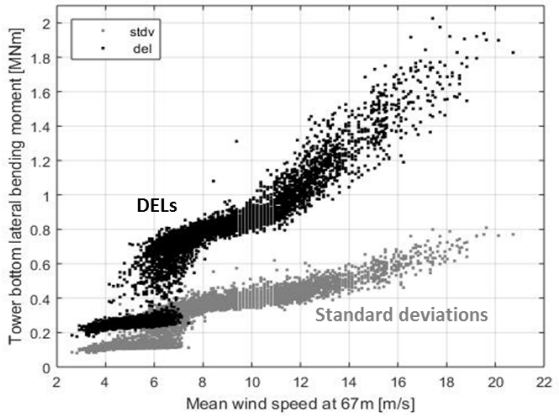

Figure 3. DELs and standard deviations of measured loads vs. wind speed for tower bottom lateral bending moment.

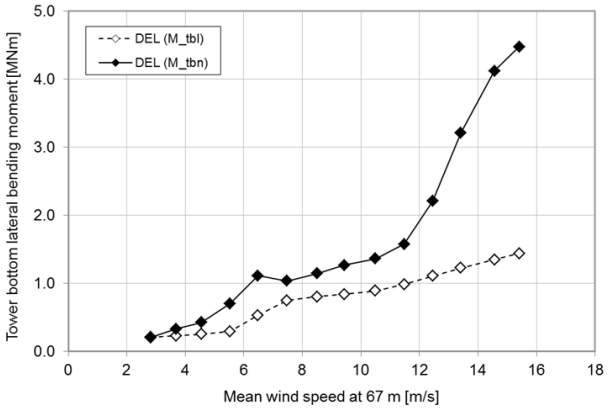

Figure 4. Bin-averaged DELs vs. wind speed for tower bottom lateral (*M_tbl*) and normal (*M_tbn*) bending moments.

3. Fatigue damage scaling method

In this section, the method for the quantification of the effect of the two neighboring wind turbines on the fatigue damage of the main components of the measured wind turbine over its entire operating time is presented.

3.1. Fatigue damage

The fatigue damage of a component, d_i, due to n_i cycles can be calculated for a load range bin, i, as follows [19]:

$$d_i = \frac{n_i}{N_i} \tag{3}$$

where N_i = number of cycles to failure for load range bin i. The total fatigue damage, D, can be determined from the sum of the i load range bins using Miner's rule [21], [22] over a given time period:

$$D = \sum d_i \tag{4}$$

For this work, equations (1) – (4) are applied as follows. Firstly, the averaged DELs from each ten-minute time series, DEL^{bin}, are calculated for all the ten-minute time series, n, in each wind speed bin:

$$DEL^{bin} = \left(\frac{\sum_{j=1}^{n} (DEL_j)^m}{n} \right)^{1/m} \tag{5}$$

In order to ensure a sufficient number of ten-minute time series for this bin-averaging, the number of time series should meet the requirements of the capture matrix according to IEC 61400-13 [1].

Secondly, the total DEL for all wind speed bins, DEL^{tot}, is calculated by summing these averaged DELs. In order to take into account the wind speed frequency distribution as well as the number of time series in each bin, the sum is weighted with a factor F_i, resulting in:

$$DEL^{tot} = \left[\sum_{i=1}^{k}\left(F_i \cdot \left(DEL_i^{bin}\right)^m\right)\right]^{1/m} \quad (6)$$

The factor F_i is defined later in sections 3.2 and 3.3. The total fatigue damage can then be written as:

$$D^{tot} = \frac{1}{C}\,(DEL^{tot})^m \quad (7)$$

Therefore in order to calculate the total fatigue damage of a component, the material property C is required. As C is not known here, ratios of increased fatigue damage in the wake and the freestream are used in order to estimate the effect of the neighboring wind turbines on the fatigue damage of the components of the measured wind turbine. This is done using in the following two steps: (1) for the measurement period, (2) extrapolation over the entire lifetime. These two steps are presented in the next sections.

3.2. Damage ratio (1): measurement period

The total fatigue damage, D, is first determined separately for the undisturbed sectors in the freestream ("free") and then for the disturbed wind conditions in the wakes of the neighboring wind turbines ("wake") using bin-averaged DELs for 1 m/s bins as follows:

$$D_{free} = \left(\frac{1}{C}\right)\sum_{i=1}^{k}\left(F_{free,i} \cdot \left(DEL_{free,i}^{bin}\right)^m\right) \quad (8)$$

$$D_{wake} = \left(\frac{1}{C}\right)\sum_{i=1}^{k}\left(F_{wake,i} \cdot \left(DEL_{wake,i}^{bin}\right)^m\right) \quad (9)$$

with $$F_{free,i} = t \cdot n_{free,i} \quad (10)$$

and $$F_{wake,i} = t \cdot n_{wake,i} \quad (11)$$

where $F_{free,i}$ is the weighting factor and $n_{free,i}$, the number of time series in the undisturbed sectors in a wind speed bin, i, and t the length of a measured time series in seconds (here 600 seconds). The weighting factor for the disturbed sectors $F_{wake,j}$ can be determined similarly, but with the number of time series in the disturbed sectors in a wind speed bin, i. As the number of measured ten-minute time series do not reach the requirements of the capture matrix at the highest wind speeds, a wind speed bin range from 2 m/s until 16 m/s is used here.

The total fatigue damage that would have occurred in the disturbed sectors if the neighboring wind turbines had not been present is then calculated from the wind speed frequency distribution in the wake and the DEL distributions in the freestream as follows:

$$D_{theo} = \left(\frac{1}{C}\right)\sum_{i=1}^{k}\left(F_{wake,i} \cdot \left(DEL_{free,i}^{bin}\right)^m\right) \quad (12)$$

The increase of actual total fatigue damage to total fatigue damage that would have occurred if the neighboring wind turbines had not been present over the measurement time is therefore calculated as follows:

$$\Delta D = \frac{D_{real}}{D_{undisturbed}} - 1 = \frac{D_{free} + D_{wake}}{D_{free} + D_{theo}} - 1 \tag{13}$$

For this calculation, the wind speed frequency distribution for operation in the wakes of the neighboring wind turbines has to be established additionally, as the nacelle anemometer does not measure the speed of the wind itself, but the speed of the wind after it has been slowed down by the neighboring wind turbines. This measurement is therefore corrected by scaling up the measured wind speed by a factor estimated using the Jensen Wake Model [23]. This model is a very simple wake model used in the most common wind park planning tools such as WindPro and WindFarmer. It assumes a linearly expanding wake with a velocity deficit depending on the distance downstream of the rotor as follows:

$$u = U_\infty \left[1 - \frac{1-\sqrt{1-C_T}}{(1+2ks)^2}\right] \tag{14}$$

where u = wind speed (m/s) at distance downstream of rotor $s = x/D$, D = rotor diameter (m), C_T = thrust coefficient of wind turbine, k = wake decay constant (assumed = 0.075). The thrust coefficient is assumed to be equal to the Enercon E-70 thrust coefficient distribution taken from a publically-available report from Overspeed GmbH [24]. The correctness or accuracy of this source cannot be checked within the scope of this work. The separate wakes of the two neighboring wind turbines as well as their combined wake were considered according to Katic [25] and the wind speed distributions were assumed to be linear from the center to the edge of the wakes.

The suitability of this correction was checked by plotting the ratio between the hub height wind speed measured by the LiDAR and the corrected nacelle wind speed vs. wind direction before and after the correction (Figure 5). For the uncorrected wind speed, in the area inside the black box, the corrected nacelle anemometer wind speed is about 30% higher than the LiDAR wind speed because the LiDAR is in the wake of the V66. In the area inside the gray box, the corrected nacelle anemometer wind speed is about 35% lower than the LiDAR wind speed because the V66 is in the wake of the neighboring wind turbines and the LiDAR is not. For the corrected wind speed, this difference is reduced from 35% to about 15%, showing that this effect has been reduced but not completely removed.

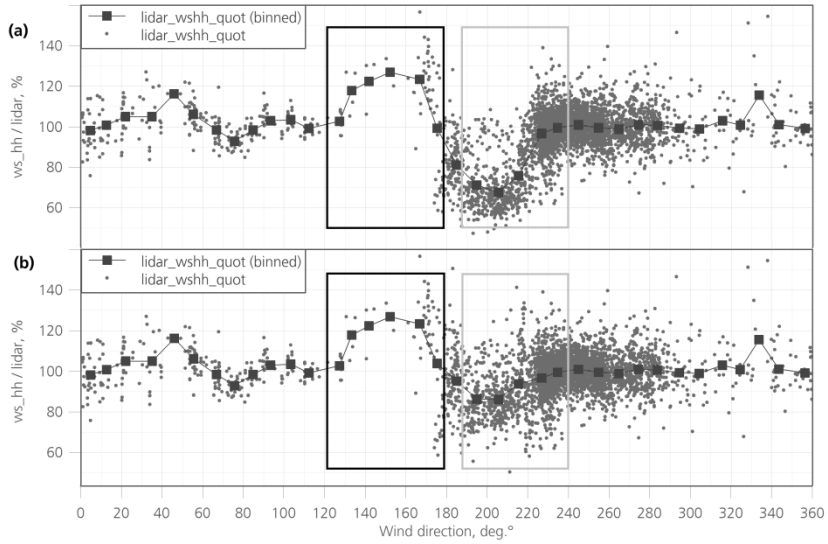

Figure 5. Ratio of hub-height wind speed measured by LiDAR to nacelle wind speed vs. wind speed for (a) uncorrected data and (b) corrected data.

3.3. Damage ratio (2): entire lifetime

Once the increase of actual total fatigue damage to total fatigue damage that would have occurred if the neighboring wind turbines had not been present has been calculated over the measurement period,

the results are then scaled up for 20 years of operation. This is done starting in December 2001, when the wind turbine was erected, and taking account for the presence of the two neighboring wind turbines since their erection in January 2006.

This is done with Miner's rule as described above, but this time by scaling the results for the typical yearly wind speed and wind direction distributions at the site. For this purpose, a further extrapolation factor is introduced, weighting the DELs according to the wind speed frequency distribution and a ratio between the design life time of 20 years and the total measurement time. The extrapolation factor in the undisturbed sectors is given for each wind speed bin, *i*, as follows [26]:

$$F_{free,i}^{life} = \frac{T_{life} \cdot A \cdot h_{v,i}}{T_{t,i}} \tag{15}$$

where T_{life} is the entire lifetime and $T_{t,i}$ is the total elapsed time of all ten-minute time series in a wind speed bin. A defines the availability of the wind turbine and $h_{v,i}$ is the frequency of the i-th wind speed bin. In the present work the availability is assumed to be 97 % and a wind speed frequency distribution according to IEC class II B [6] is assumed to be applicable for the entire 20 years, because this wind speed distribution is typical for the investigated wind farm site. The extrapolation factor $F_{wake,i}^{life}$ is determined for the disturbed sectors similarly, but according to the time series in the disturbed sectors.

The total fatigue damage over the entire lifetime is then determined based on the previously calculated bin-averaged DELs and the extrapolation factor. Using equations (8) to (13) and replacing the weighting factor with $F_{free,i}^{life}$, the total lifetime fatigue damage is calculated as follows:

$$D_{free}^{life} = \left(\frac{1}{C}\right) \sum_{i=1}^{k} \left(F_{free,i}^{life} \cdot \left(DEL_{free,i}^{bin}\right)^{m}\right) \tag{16}$$

$$D_{wake}^{life} = \left(\frac{1}{C}\right) \sum_{i=1}^{k} \left(F_{wake,i}^{life} \cdot \left(DEL_{wake,i}^{bin}\right)^{m}\right) \tag{17}$$

$$D_{theo}^{life} = \left(\frac{1}{C}\right) \sum_{i=1}^{k} \left(F_{wake,i}^{life} \cdot \left(DEL_{free,i}^{bin}\right)^{m}\right) \tag{18}$$

where D_{free}^{life} and D_{wake}^{life} are the summed fatigue damages of all wind speed bins over the entire lifetime in the undisturbed and disturbed sectors, respectively. D_{theo}^{life} is defined as the "theoretical" fatigue damage if the two neighboring wind turbines had not been present.

Thus, taking into account the five years in which the measured wind turbine was not disturbed by the neighboring wind turbines together with the fifteen years in which it is disturbed, the total fatigue damage for the real situation is then given by:

$$D_{real}^{life} = D_{free,5y}^{life} + D_{theo,5y}^{life} + D_{free,15y}^{life} + D_{wake,15y}^{life} \tag{19}$$

Then for the theoretical situation if the neighboring wind turbines would not be present:

$$D_{undisturbed}^{life} = D_{free,20y}^{life} + D_{theo,20y}^{life} \tag{20}$$

The increase of actual total fatigue damage to total fatigue damage that would have occurred if the neighboring wind turbines had not been present over the entire lifetime is therefore calculated as follows:

$$\Delta D^{life} = \frac{D_{real}^{life}}{D_{undisturbed}^{life}} - 1 \tag{21}$$

4. Fatigue damage results

4.1 Increase in damage over measurement period

The increase in total fatigue damage of each component due to the presence of the neighboring wind turbines over the measurement period, ΔD^{life}, is shown in Figure 6. This shows an increase in damage between 2.5% and 104% due to the presence of the neighboring wind turbines, depending on the component. The rotor blade flatwise bending moment is affected the most by the neighboring wind turbines, showing that the blade is much more sensitive to the increased turbulence in the wake than the edgewise direction, as expected, because the edgewise bending moment is mainly dependent on gravitational forces. Furthermore, the main shaft and tower top torsion are also strongly affected by the neighboring wind turbines due to the direct transfer of the flatwise bending moment fluctuations from the blades. The comparably small increase in fatigue damage of the tower bottom compared to the tower top bending moments indicate that the increase in tower top bending moments also originate directly from the blade flatwise bending moment and not directly from the fluctuating forces on the tower itself.

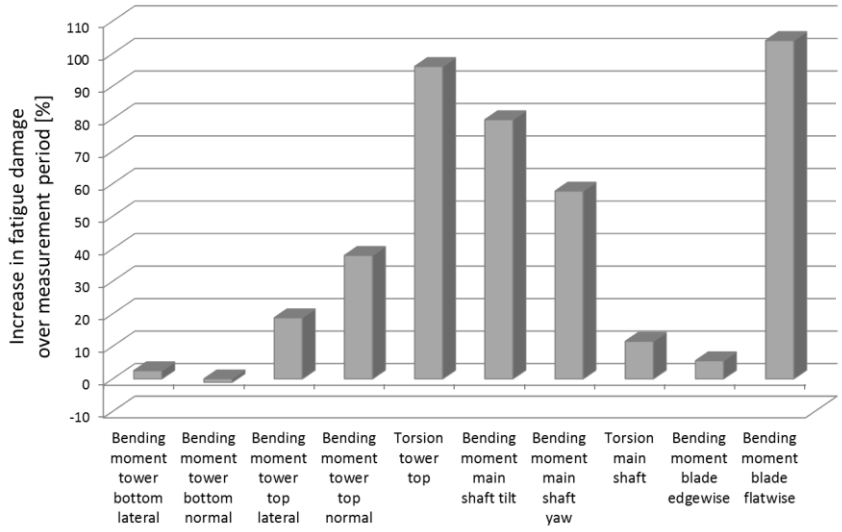

Figure 6. Increase in total fatigue damage due to the neighboring wind turbines over the measurement period.

4.2 Increase in damage over entire lifetime

The increase in total fatigue damage of each component due to the presence of the neighboring wind turbines over 20 years, D_{ratio}^{life}, is shown in Figure 7. The increase in total fatigue damage over the entire lifetime is approximately between 3% and 65%, except for the tower bottom normal bending moment (discussed below). As expected, a similar behavior of the damage increase can be seen as for the results from the measurement period; the rotor blade flatwise bending moment and the tower top torsion are affected most by the neighboring wind turbines. However, the overall damage increase is lower. This is because the peak of the IEC class II B wind speed frequency distribution [6] used here occurs at a lower wind speed than the wind speed frequency distribution over the measurement period.

The negative value of approximately -15% for the tower bottom normal bending moment mentioned above means that the fatigue damage without the presence of the neighboring wind turbines is larger than the damage caused with the neighboring wind turbines. As this does not seem to be particularly likely, the quality of the method is investigated in the next section.

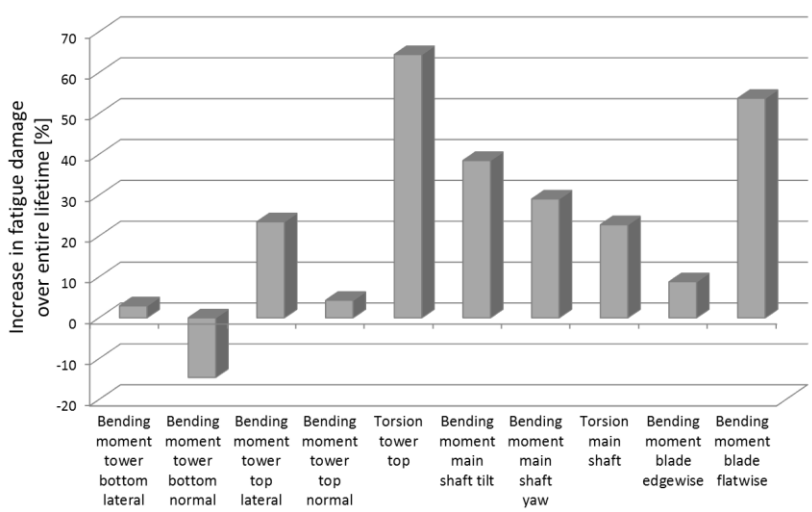

Figure 7. Increase in total fatigue damage due to the neighboring wind turbines over the entire lifetime.

5. Evaluation of method

A method for quantifying the effect of neighboring wind turbines on the fatigue damage of the main components of a measured wind turbine over its entire operating time using short-term load measurements has been introduced in this work. The method has been applied to a real case and the results appear to be plausible. Furthermore, the results show that the increase in total lifetime fatigue damage due to neighboring wind turbines for wind turbine separations of the order of 5*D* is significant and needs to be taken account of in wind farm planning software. However, if this method is to be used in the future for improving wake models or for lifetime extension calculations, the accuracy needs to be investigated. This is done here by considering the main assumptions.

5.1 Main assumptions

The main assumptions thought to be relevant for the method accuracy are:

1. The results are assumed to be independent of the number of ten-minute time series in a wind bin, as long as there are enough time series to meet the IEC 61400-13 requirement.
2. An IEC wind speed frequency distribution is assumed for the site.
3. The wind speed frequency distribution is assumed to remain constant over 20 years.
4. Extreme loads and operating conditions other than normal operation are disregarded.
5. The variation of turbulence intensity with wind speed as well as other effects such as wind shear and veer are assumed to be the same over 20 years as over the measurement period.
6. The behavior and performance of the neighboring wind turbines is assumed to be the same over 20 years as over the measurement period.

These assumptions and their impact on the accuracy of the method are discussed below.

5.1 Assumption 1

Assumption 1 can be used to explain the anomalous result in Figure 6 for the tower bottom normal bending moment as follows.

Figure 8 depicts the DELs for the tower bottom normal bending moment. Each point refers to a DEL for one ten-minute time series for the undisturbed (“free”, black) and disturbed sectors (“wake”, gray). The crosses show the bin-averaged DELs over the wind speed bins (plotted with lines in order to increase the readability and to show the trend of the DELs). A sudden increase in the bin-averaged DELs between 4 m/s and 7 m/s can be seen due to the separate point cloud at higher DEL values in this wind speed range (circled on the plot). This occurs because the wind speed and thus the rotational speed of the rotor are located in a region where the generator switches from the first to the second

generator stage, increasing the fatigue damage. The bin-averaged DELs in the wake (gray line) appear to be higher than the bin-averaged DELs in the freestream (black line) due to the larger number and higher values of the different ten-minute time series in these wind speed bins.

Further evidence for the dependency of the DELs on the number of ten-minute time series can be seen in Figure 8 at wind speeds above 14 m/s. In this wind speed range, the number of ten-minute time series is so low that the averages cannot be reliably calculated.

This shows that the results are dependent on the number of ten-minute time series in a bin. A standard number of ten-minute time series for the bin-averaging of the DELs thus needs to be established before this method is applied for improving wake models or for lifetime extension calculations. This is being carried out presently.

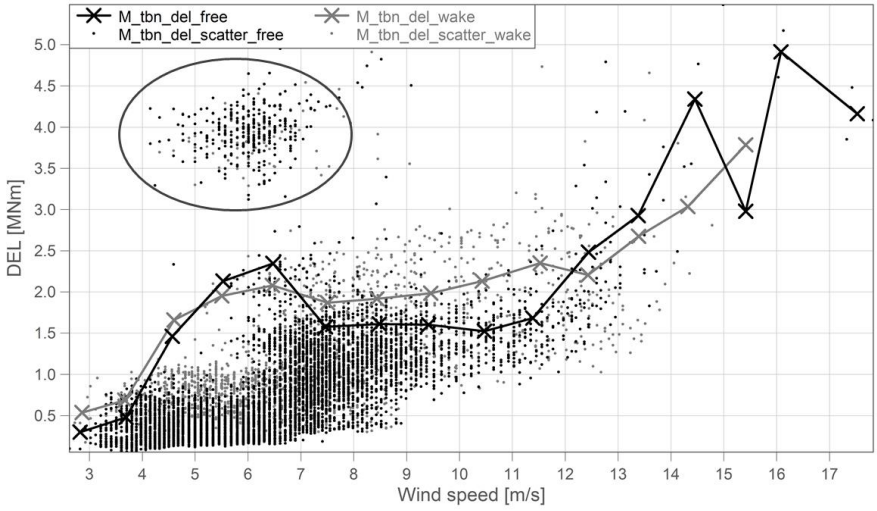

Figure 8. Bin-averaged DELs (black and gray lines with crosses) and scatter plot DELs from ten-minute time series over wind speed bins for tower bottom normal bending moment.

5.1 Assumptions 2 and 3

The impact of assumption 2 on the results is investigated here by carrying out the calculations for three different wind speed frequency distributions. Step (2) of the method is undertaken for wind speed frequency distributions according to IEC wind classes I, II and III [6].

The results are depicted in Figure 9, showing the effect of the different wind speed frequency distributions on ΔD^{life}. It can be seen that the tower top torsion, the bending moments of the main shaft and the rotor blade flatwise bending moment are especially affected by the different frequency distributions. For all components except the main shaft torsion, the damage increase gets larger as the wind speed frequencies in the lower bin range increase. For the main shaft torsion, the damage increase reduces with increasing wind speed frequency in the lower bin range, showing that the effect of the influence of higher wind speeds is larger than the influence of the higher frequency in the lower bin range.

This high dependency of the wind speed frequency distribution on the results indicates that the choice of wind speed frequency distribution needs to be standardized for the method. The accuracy would be improved if the measured wind speed frequency distribution from the specific wind farm site would be used for the extrapolation over the entire lifetime. Furthermore, it indicates that assumption 3 also has an influence on the results. The accuracy of the method could be improved further by using a long-term extrapolation of the wind speed, for example based on the standard wind resource assessment guidelines [27].

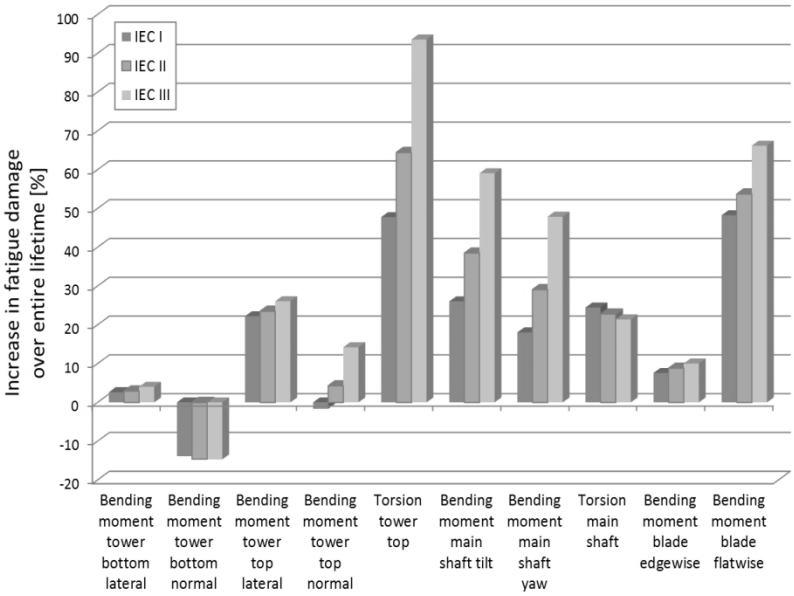

Figure 9. Increase in total fatigue damage over the entire lifetime due to different wind speed frequency distributions (IEC wind class I, II, III) for each component.

5.1 Assumptions 4-6

These assumptions are also expected to have an influence on the accuracy of the results. However, the sensitivity of these assumptions on the results cannot be calculated within the scope of this work and require further investigation. This is being undertaken presently.

6. Conclusions

- A method has been developed for quantifying the effect of neighboring wind turbines on the fatigue damage of the main components of a wind turbine over its entire operating time using short-term load measurements.
- The method was applied to a measurement campaign on a Vestas V66 wind turbine located in northern Germany and the results were found to be plausible.
- Furthermore, the results have shown that the increase in total lifetime fatigue damage due to neighboring wind turbines for wind turbine separations of the order of 5*D* is significant and needs to be taken account of in wind farm planning software.
- The accuracy of the method has been examined by investigating the sensitivity of the main assumptions on the results. A strong dependency on the number of measured time-series in a wind speed bin as well as on the choice of wind speed frequency distribution was found.
- This method could be used in the future for improving wind farm planning software by taking into account fatigue damage as well as energy yield or for improving lifetime extension calculations of wind turbines. However, in order to do this, the assumptions need to be further investigated and the method standardized.

References

[1] 2015 *International standard IEC 61400-13: Wind turbines – Part 13: Measurements of Mechanical Loads*
[2] 2013 *Kostensituation der Windenergie an Land in Deutschland* (Deutsche Windguard)
[3] Damaschke M, Illig C, Stache F and Baumjohann F 2004 *DEWEK Proceedings*
[4] www.emd.dk; Accessed 10-June-2016
[5] www.dnvgl.com; Accessed 10-June-2016
[6] 2005 *International standard IEC 61400-1: Wind turbines – Part 1: Design requirements*
[7] Seifert H, Kröning J 2003 *EWEC* Madrid, Spain

[8] 2012 *Richtlinie für Windenergieanlagen: Einwirkungen und Standsicherheitsnachweise für Turm und Gründung* Deutsches Institut für Bautechnik, Berlin
[9] Samorani M 2013 *Handbook of Wind Power Systems* (Heidelberg: Springer Berlin) pp 21–38
[10] Frandsen S and Thogersen ML 1999 *Wind Eng*. **23(6)** 327–40
[11] Vermeer LJ, Sorensen JN and Crespo A 2003 *Progress in Aerospace Sciences* **39** 467–510
[12] Faerron R, Lott S, Müller K and Cheng PW 2015 *RAVE International Conference* Bremerhaven, Germany
[13] 2015 BWE-Serviceumfrage
[14] DNVGL-ST-0262 2016
[15] Kamieth R, Liebich R, Heilmann C, Melsheimer M and Grunwald A 2015 *6. VDI-Fachtagung Schwingungen von WEA* Bremen, Germany
[16] 2007 *International standard IEC 61400-12-1: Wind turbines – Part 12-1: Power Performance Measurements of Electricity Producing Wind Turbines*
[17] Barber S, Mechler S and Maas O 2015 *Poster presentation EWEA 2015* (Paris)
[18] 2014 *International standard IEC 61400-12-2: Wind turbines – Part 12-2: Power Performance Measurements of Electricity Producing Wind Turbines Based on Nacelle Anemometry*
[19] Woehler A, 1870 *Zeitschrift fuer Bauwesen* **20** pp 73-106
[20] Madsen P 1990 *Executive Committee of the International Agency Programme for Research and Development on Wind Energy Conversion Systems* **2**
[21] Palgrem A 1924 *VDI-Zeitschrift* p 339
[22] Miner A 1945 *J. Appl. Mech. Trans. ASME* **12** 159-64
[23] Jensen N 1983 *RISO-M-2411* (Riso National Laboratory, DK-4000 Roskilde, Denmark)
[24] http://www.bodenkontor-steinhoehe.de/pdf/Anlage_44_Windenergie.pdf; Accessed 17-August 2016
[25] Katic I, Højstrup J and Jensen NO 1986 *European Wind Energy Association Conference and Exhibition* Rome, Italy.
[26] *NWTC Information Portal (MLife)*, http://nwtc.nrel.gov/MLife. Last modified 30-October-2015; Accessed 10-June-2016
[27] 2014 *Technische Richtlinien für Windenergieanlagen: Teil 6 Bestimmung von Windpotenzial und Energieertraegen* **9** (Fördergesellschaft Windenergie und andere Erneuerbare Energien)

Acknowledgements
This project was funded by the Federal State of Bremen and the European Regional Development Fund.

Thanks also to project partners *Projektierungsgesellschaft für regenerative Energiesysteme mbH* and the research group *fk-wind:* of the University of Applied Sciences Bremerhaven.